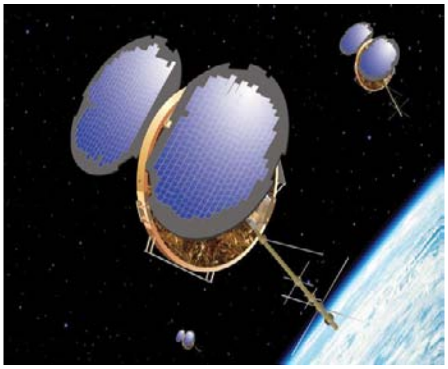

COSMIC

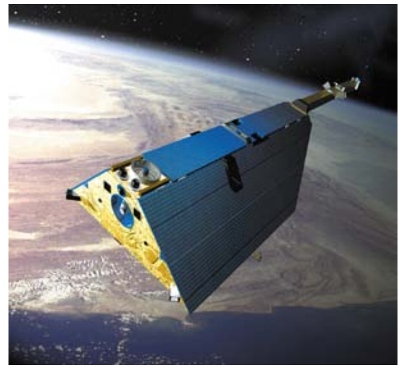

CHAMP

YEAR 3 ANNUAL PROJECT REPORT
NOAA GRANT NA07OAR4310224

VALIDATION AND CALIBRATION OF MSU/AMSU MEASUREMENTS AND RADIOSONDE OBSERVATIONS USING GPS RO DATA FOR IMPROVING STRATOSPHERIC AND TROPOSPHERIC TEMPERATURE TREND ANALYSIS

Principal Investigator:
Shu-peng Ben Ho (303-497-2922, spho@ucar.edu)

Co-Investigators:
Cheng-Zhi Zou ((301) 763-8042 x156, cheng-zhi.zou@noaa.gov)
Ying-Hwa Kuo **(**(303) 497-8910, kuo@ucar.edu)

National Center for Atmospheric Research
P.O. Box 3000, Boulder CO 80307, USA

1. Introduction

The monitoring and detecting of the vertical structure of atmospheric temperature trends are key elements in the climate change problem. Over the past decade, the roughly 30 years of the combined Microwave Sounding Unit (MSU) and Advanced Microwave Sounding Unit (AMSU) measurements have been extensively used for climate temperature trend detection. Nonetheless, due to different adjustments and analysis procedure used to calibrate shift of sensor temperature owing to on-orbit heating/cooling of satellite components and inter-calibration for MSU/AMSU measurements from different missions, large trend differences were found between different groups. Radiosondes are the only operational instruments that have provided continuous atmospheric pressure, temperature, and humidity measurements in the troposphere and lower stratosphere (~25 km) for more than three decades. However, because the quality of radiosonde measurements varies with height and instrument types, air temperature trends constructed from radiosonde measurements are subject to significant uncertainty.

The Global Positioning System (GPS) Radio Occultation (RO) technique has been proven to be a mature global observation technique and is ideally suited for climate trend detection. GPS RO produces global data coverage without the need for calibration or bias correction. Because GPS RO data do not contain orbit drift errors and are not affected by on-orbit heating and cooling of the satellite component, they are very useful to identify the MSU/AMSU time/location dependent biases for different NOAA missions and to assess systematic radiosonde biases.

The specific goals for this project are as followings:

- **Task 1: Using GPS RO data to help identify a set of operational radiosonde network for further climate studies.**

- **Task 2: Using GPS RO data in the stratosphere and the identified radiosondes in the troposphere as climate benchmark datasets to validate MSU and AMSU measurements to understand exactly how and why there are differences in temperature trends reported by several analysis teams using the same observation systems but different analysis methods.**

- **Task 3: Generating long-term stratospheric and tropospheric climate quality temperature datasets by reprocessing nine years of AMSU/MSU data from 2001 to 2009 and delivering this data set to NCDC.**

The work undertaken to date on these project goals is detailed in section 2 and immediate plans are detailed in section 3. This is the third year of this proposed study. Most of the proposed tasks are completed. However, due to the evolving nature of this study and practical difficulties to transferring the analysis codes and data to NCDC, we feel that we better extend some of the proposed tasks (documentation and data/code transferring) and prolong the possible transferring processes into year 4. We plan to start to work with NCDC experts as soon as they are identified, and will work with them continuously in year 4 till all data and computer codes are completely transferred. More details of plans for year 4 will be addressed in section 4.

2. Progress on Proposed Studies

In this study, we propose to use MSU/AMSU measurements, radiosonde observations, and GPS RO data from *Challenging Minisatellite Payload* (CHAMP) from 2002 to 2009 and FORMOSAT-3/Constellation Observing System for Meteorology, Ionosphere, and Climate mission (denoted as COSMIC hereafter) from 2006 to 2009 to construct consistent long-term stratospheric and tropospheric climate quality temperature datasets. Following tasks in year 2, **work to-date has focused on 1) continuing the preparation of GPS RO, radiosonde and MSU/AMSU data for geo-location comparisons, 2) continuing to quantify the uncertainty of GPS RO data for climate monitoring, 3) continuing to estimate the reproducibility for using GPS RO data for climate monitoring, 4) continuing the assessment of the systematic temperature biases of global radiosonde measurements using RO data, 5) continuing the assessment of the systematic water vapor biases of global radiosonde measurements using RO data, 6) construction of a consistent microwave sensor temperature record in the lower stratosphere using GPS RO data and microwave sounding measurements, and 7) comparisons of CHAMP/COSMIC, RSS, UAH, and SNO TLS Trends.**

2.1 Preparation of GPS RO, Radiosonde, and MSU/AMSU Data for Geo-location Comparisons

Several new processed GPS RO data, NOAA MSU/AMSU data, MSU/AMSU climatology from RSS and UAH groups, AMSU data from NASA Aqua AMSU measurements, and temperature measurements from global radiosondes are collected. Two procedures were performed to prepare the data for further comparisons:

a. Data collection (all data we have collected, newly processed data are in blue)

We downloaded the following data from corresponding FTP and achieve sites:

- CHAMP data (from Jan. 2001 to April 2010) from UCAR CDAAC,

- COSMIC data (from June 2006 to April 2010) from UCAR CDAAC,
- GRACE data (from June 2006 to Dec. 2008) from UCAR CDAAC,
- MSU/AMSU data from NESDIS ($NESDIS_{OPR}$) for NOAA 14 (MSU), NOAA 15 (AMSU), NOAA 16 (AMSU) and NOAA 18 (AMSU) from 2002 to 2010,
- RSS V3.2 data from 2001 to 2009 from their FTP site,
- UAH V5.1 data from 2001 to 2009 from their FTP site,
- New processed $NESDIS_{NEW}$ V2.0 data (processed by Dr. Cheng-Zhi Zou and NOAA team) from their related FTP sites,
- Global radiosonde data from NCAR archive, and
- ECMWF data from NCAR archive.

b. Data matching

To minimize the temporal/spatial/vertical-resolution mismatches among various datasets, we generated the following collocated data pairs:

- CHAMP-COSMIC, GRACE-COSMIC pairs (within 90 minutes, and 200 km).
- MSU/AMSU-RO pairs (within 15 minutes, and 50 km).
- RSS/UAH-RO pairs (monthly mean, 2.5×2.5 grid, we further bin each monthly mean MSU/AMSU and CHAMP 2.5 degree × 2.5 degree matched pairs into 10 degree × 10 degree grids).
- Radiosonde-RO pairs (temperature and moisture profiles obtained from radiosondes are interpolated onto RO locations within 3 hours and 200 km).
- ECMWF-RO pairs (ECMWF temperature and moisture profiles are interpolated onto RO locations within 3 hours and 200 km).
- To avoid AMSU vertical weighting function representation errors, instead of using a global fixed weighting function (WF), we apply a COSMIC/CHAMP dry temperature profile to an AMSU fast forward model from the Cooperative Institute for Meteorological Satellite Studies-CIMSS with 100 fixed pressure levels.

2.2 Continue to Quantify the Uncertainty of GPS RO Data for Climate Monitoring

To use GPS RO data for climate monitoring, we need to quantify their precision, long term stability and reproducibility.

a. ***Quantification of the Precision of COSMIC Data for Climate Studies***

- **Here we continue to quantify the precision of GPS RO data by comparing RO data with those from European Centre for Medium Range Forecasts (ECMWF) analysis:** we perform a global comparison of temperature and water vapor profiles from the collocated COSMIC and ECMWF analysis. ECMWF analysis represents optimal temperature and humidity estimates from high quality observations among multi-satellite sounders, imagers, and conventional in situ observations including radiosondes through a data assimilation system. Results show that COSMIC temperature retrievals are highly consistent with those from ECMWF globally with a close to zero mean (He et al**.,** 2009). When compared with water vapor (WV) profiles from global ECMWF analysis, the individual COSMIC RO profiles of specific humidity yield an accuracy of less than 0.05 g/kg above 2 km, and less than 0.2 g/kg below 2 km (Ho et al., 2010a). Papers summarizing these results are listed in Section 2.8.
- **Comparing results from COSMIC FM3 -FM4 dry temperature:** this is to further quantify the possible cause of temperature difference in different latitudinal zones received from two COSMIC receivers. **Figure 1** shows that the mean dry temperature differences between two COSMIC receivers are very close to zero for each 10 degree latitudinal bin.

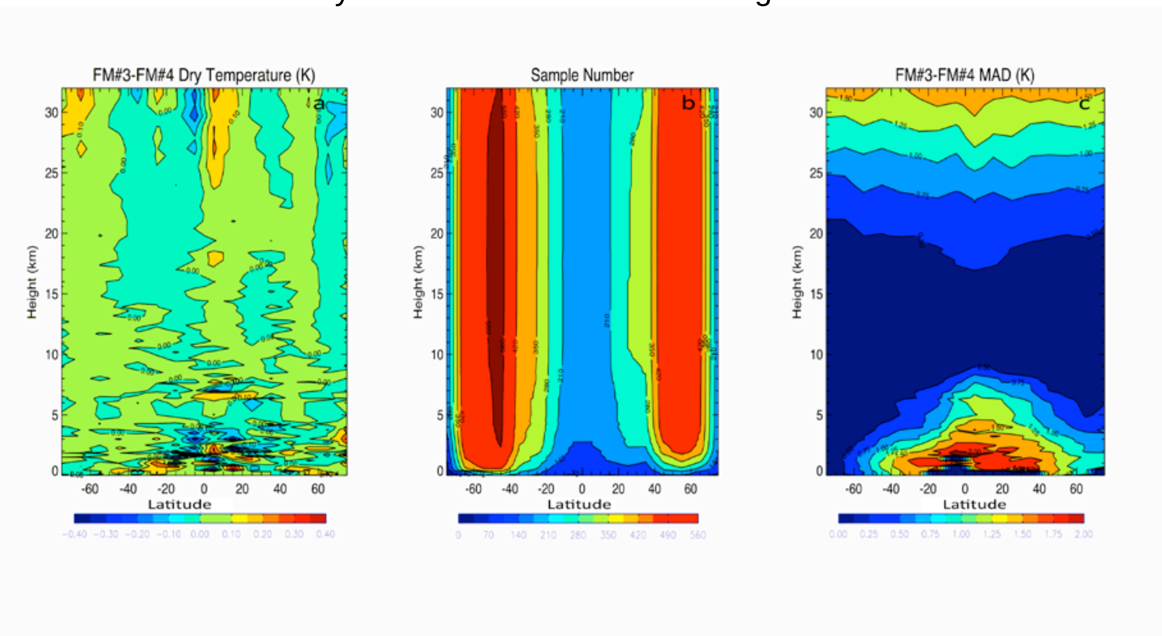

Figure 1. (a) mean FM3-FM4 dry temperature difference for each 10 degree latitudinal bin, (b) the sample number used for each 10 degree latitudinal bin for this comparison, (c) the FM3-FM4 Median Absolute Difference (MAD).

b. Continue to Quantify the Long-term Stability among different RO Missions

Here we continue to quantify the differences of inverted profiles among different RO missions which were launched in different years. This is to demonstrate the long-term stability of RO data for climate monitoring.

- **Collect atmospheric soundings from multi-RO missions including SAC-C, GRACE, CHAMP, COSMIC, and MetOp-A GRAS, which are all processed by UCAR:** we used the latest post-processed SAC-C, GRACE, CHAMP, COSMIC, and MetOp-A GRAS data from 2001-2009 to quantify the mean difference among different RO missions in order to demonstrate that the quality of GPS RO data will not change after launch.
- **Compare collocated profiles from two RO missions for similar azimuth angle, close time, close distances. Only high quality RO data are used in the comparison.**
- **Compare RO profiles of high signal to noise ratio (SNR) between COSMIC and MetOp-A GRAS temperature profiles:** This is to demonstrate the quality of COSMIC data above 25 km (from 25 km to 40 km). RO profiles from MetOp-A GRAS contain better SNR than those from COSMIC. **Figure 2** show that those high SNR COSMIC profiles above 25 km are of the same quality to those from GRAS, where its mean bias from 12 km to 40 m is equal to -0.05 K.

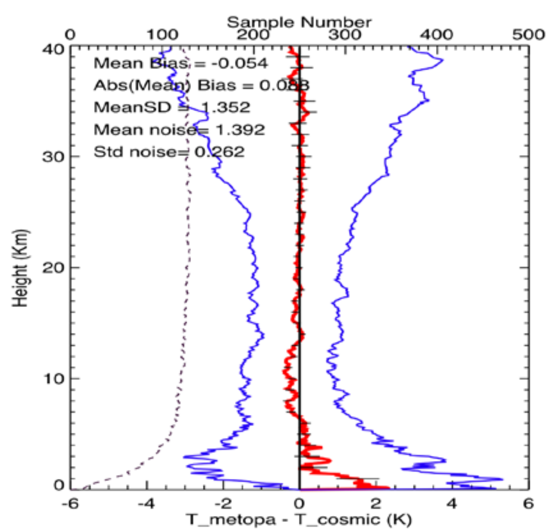

Figure 2. METOPA-COSMIC in 90S-90N in 250 km and 90 minutes where COSMIC profiles with standard deviation noise (defined as $\sigma_{obs} = \sqrt{\langle(\alpha - \alpha_{guess})^2\rangle}$) smaller than 3x10^(-6) were used.

2.3 Estimates of the Reproducibility for using GPS RO Data for Climate Monitoring: Inter-comparisons of Refractivity Derived from Different Data Centers

Before using GPS RO data for climate monitoring, we need not only to quantify the precision and long-term stability of GPS RO data but also to quantify the dependence of errors in GPS RO-derived variables on atmospheric excess phase processing and inversion procedures. Currently, multi-year of GPS RO climate data can be obtained from the GeoForschungsZentrum Potsdam (GFZ), Germany, the Jet Propulsion Laboratory (JPL), Pasadena, CA, USA, the University Corporation for Atmospheric Research (UCAR), Boulder, CO, USA, and the Wegener Center of the University of Graz (WegC), Graz, Austria, Danish Meteorological Institute (DMI), Copenhagen, Denmark, and EUMETSAT (EUM). Different centers used different assumptions, initializations, and implementations in the excess phase processing and inversion procedures, which may introduce refractivity differences between centers.

- **The profile-to-profile refractivity comparison between UCAR, JPL, WegC, GFZ, EUM, and DMI are compared:** Note that because different implementations of quality control have the effect of eliminating different subsets of the entire data set, the previous MMC comparisons in Ho et al. (2009c) still contain sampling errors for different centers. To quantify the structural errors of RO data processed by different centers, we conduct the profile-to-profile refractivity comparison. **Figure 3** shows that the mean profile-to-profile fractional refractivity difference between UCAR and DMI is less than 0.06% in the height between 12 km and 25 km, with a standard deviation less than 0.21%. The mean profile-to-profile fractional refractivity difference between UCAR and other centers are all less than 0.06% except that for GFZ. The GFZ-UCAR fractional refractivity difference is equal to 0.17% with a standard deviation of 0.22%.

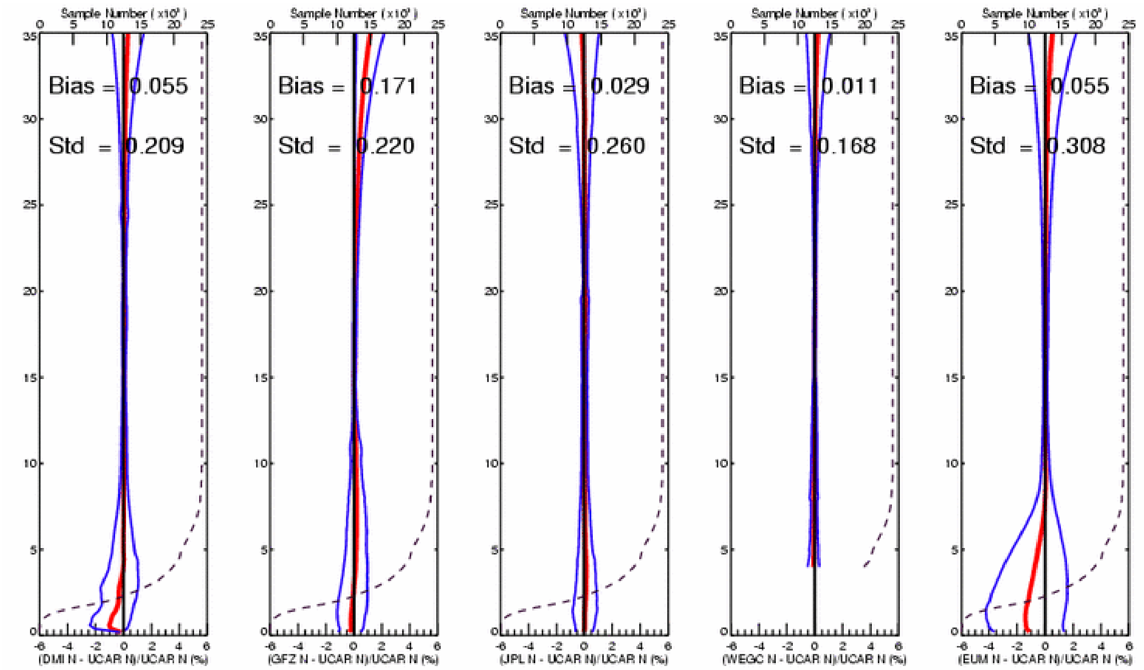

Figure 3. The global profile-to-profile fractional refractivity comparison for 2002 between (a) DMI and UCAR (the most left panel), (b) GFZ and UCAR (the second panel from the left), (c) JPL and UCAR (the middle panel), (d) WegC and UCAR (the fourth panel from the left), and (e) EUM and UCAR (the most right panel).

2.4 Assessment of the Systematic Biases of Global Radiosonde Temperature Measurements using RO Data

Because the quality of COSMIC RO data are not affected by the surrounding environment (e.g., geo-location, day and night, etc.), GPS RO data are very useful to identify the possible radiative biases of radiosondes, where sensor characteristics vary considerably in times and locations for different sensor types.

- **Quantify the radiative effect on radiosonde temperature anomalies using COSMIC temperature profiles:** The quality of radiosonde temperature measurements varies obviously by day and night for different radiosonde sensor types. Here we compare temperature profiles derived from GPS RO data of the COSMIC mission with those from four types of radiosonde systems from 10 to 25 km to assess the performance of these radiosonde systems in the upper troposphere and lower stratosphere. Results show that temperature measurements from Vaisala-RS92 and Shanghai radiosonde systems agree well with those of COSMIC with a close-to-zero mean difference. Large temperature biases are shown for MRZ and VIZ-B2 radiosonde systems relative to COSMIC, which are possibly caused by diurnal radiative effects. These biases and their possible causes are consistent with previous studies. In addition, we show that the temperature measurements from the new Chinese radiosonde system can be improved through a comparison with COSMIC measurements. Results from this study are summarized in He et al., (2009). Only radisonde temperature profiles from 2006 June to 2007 February were used.
- **Extend the comparison of GPS RO temperature profiles and radisodne comparison from 2002 to 2008**: Here we compare temperature profiles derived from GPS RO data from the COSMIC from 2006 to 2008 and CHAllenging Minisatellite Payload (CHAMP) from 2002 to 2008 with those from different types of radiosonde systems from 12 to 25 km to assess the performance of these radiosonde systems in the upper troposphere and lower stratosphere. Because GPS RO data are not affected by the temperature variation of the satellite component, we are also able to identify the radiosonde temperature biases due to possible radiative errors resulting from instrument characteristics for different types of radiosonde systems. Because of different solar absorptivity and infrared emissivity, different radiosonde sensor systems actually contain different radiative biases. **Figure 4** shows GPS RO temperature profiles are very useful to identify systematic radiative biases for different radiosonde sensor types**.**

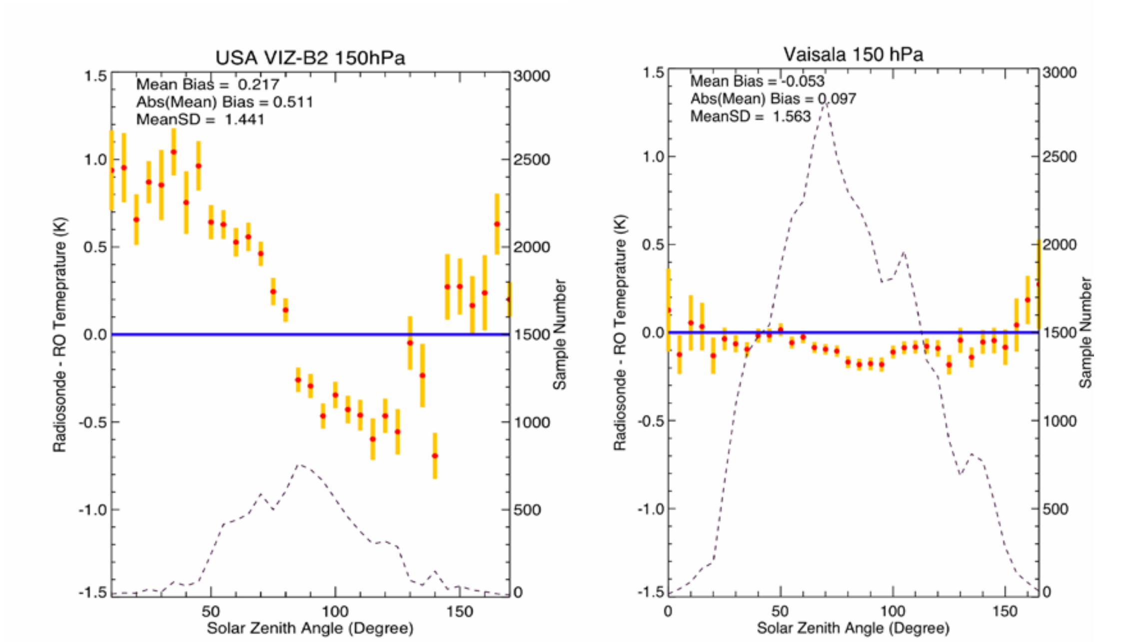

Figure 4. Temperature comparisons between COSMIC and radiosonde at 150 hPa for (a) USA VIZ-B2 (the left panel), and (b) Vaisala-RS92 (the right panel) from 2002 to 2008. The red dot is for the mean difference, the orange line is for the standard deviation, and the dotted line is the sample number for RO and radiosonde pairs in that height.

2.5 The Usefulness of COSMIC Data to Assess the Water Vapor Biases of Different Types of Radiosonde Systems

Because in the lower troposphere RO data are very sensitive to water vapor variation than that of temperature, the ROs yield profiles of all-weather humidity in a 200 km horizontal resolution accurate to 0.2 to 0.5 g/kg in the lower to middle troposphere. Here we use RO water vapor in the lower troposphere to assess the water vapor biases of different types of radiosonde systems.

- **Matching COSMIC water vapor profiles with those radiosonde water vapor profiles:** To assess the systematic water vapor biases measured from different types of radiosonde systems, we conducted comparisons of water vapor profiles derived from COSMIC and those profiles of radiosondes over Russia, Japan, China, and India. Radiosonde temperature measurements within 2 hours and 300 km of COSMIC RO soundings are used to compare to those from COSMIC.
- **Compare COSMIC water vapor profiles with those from ECMWF**: To quantify the accuracy of the estimated COSMIC refractivity and water vapor profiles, we also compared COSMIC profiles to those from the European Centre for Medium Range Forecasts (ECMWF) global analysis over the same geographical area of radiosondes during the same period. Results show that the quality of the RO soundings is very consistent over different geographical areas. This is evidenced by the relatively small variations in the COSMIC and ECMWF water vapor differences between geographical areas.
- **Assess the systematic water vapor biases measured from different types of radiosonde systems using COSMIC water vapor data:** on the contrary to the RO-ECMWF water vapor comparison results, COSMIC-Radiosonde water vapor biases (in g/kg) vary considerably for different areas. There are obvious dry water vapor biases for those radiosondes from China (**Figure 5**) and India (not shown) where there are no obvious radiosonde water vapor biases from Russia and Japan. Results here demonstrate the usefulness of COSMIC-derived water vapor profiles to assess the systematic water vapor biases from different types of radiosonde systems.
- Results found in this study was submitted to Remote Sensing (**Ho, S.-P.**, Xinjia Zou, Y.-H., Kuo, 2010: Assessment of the Quality of Radiosonde in the Troposphere using GPS Radio Occultation from COSMIC, *Remote Sensing*).

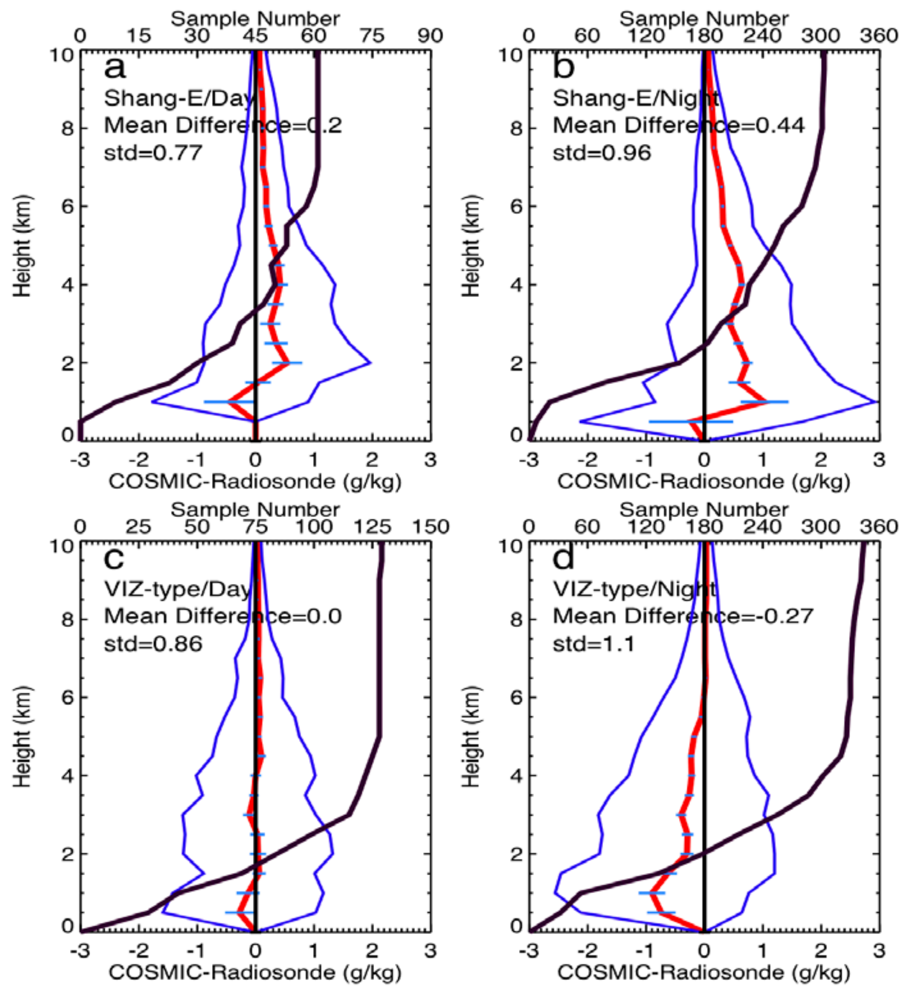

Figure 5. The same as Figure 3 except for (a) COSMIC-Shang-E ensembles during the day, (b) COSMIC-Shang-E ensembles during the night, (c) COSMIC-VIZ-type ensembles during the day, and (d) COSMIC-VIZ-type ensembles during the night.

2.6 Construction of a Consistent Microwave Sensor Temperature Record in the Lower Stratosphere Using Global Positioning System Radio Occultation Data and Microwave Sounding Measurements

In this study, we use COSMIC data and CHAMP data to simulate Advanced Microwave Sounding Unit (AMSU) brightness temperatures for the lower stratosphere (TLS) and compare them to AMSU TLS from different National Oceanic and Atmospheric Administration (NOAA) missions from January 2002 to Dec. 2008. RO TLS is used to calibrate NOAA AMSU TLS. Then the RO-consistent AMSU TLS from NOAA 15, 16, and 18 are used to construct a consistent microwave sensor temperature record in the lower stratosphere.

Our analysis shows that because RO data do not contain mission-dependent biases and orbit drift errors, and are not affected by on-orbit heating and cooling of the satellite component, they are very useful to identify the AMSU time/location dependent biases for different NOAA missions. Using RO simulated AMSU Tbs, we calibrate AMSU TLS from different NOAA missions in the same month. A new microwave sensor temperature record in the lower stratosphere from 2002 to 2008 is constructed. The derived TLS record is compared with the newly available TLS datasets provided by Remote Sensing Systems (RSS) and University of Alabama in Huntsville (UAH). The causes of the TLS differences among these datasets are discussed in Section 2.7.

Approaches:

1) Data:
    COSMIC from 200606 to 200912
    CHAMP from 200106 to 200806
    RSS V3.2 200106-200912
    UAH V5.1 200106-200812
    SNO V2.0 200106-200912

2) Apply CHAMP and COSMIC soundings to AMSU forward model to simulate AMSU TLS

3) Match simulated GPS RO TLS to NOAA AMSU TLS within 30 minutes and 0.5 degree to find calibration coefficients for different NOAA satellites so that we can

    a. Use GPS RO data to inter-calibrate other NOAA satellite.
    b. Use the NOAA satellite measurements calibrated by GPS RO data to calibrate multi-year AMSU/MSU data and generate consistent RO and MSU/AMSU TLS climate data records.
    c. The derived TLS record is compared with the newly available TLS datasets provided by Remote Sensing Systems (RSS) and University of Alabama in Huntsville (UAH).

The monthly 2.5x2.5 gridded AMSU TLS from UAH, RSS, RO-calibrated TLS, and those calibrated using NOAA SNO methods are shown in **Figure 6**.

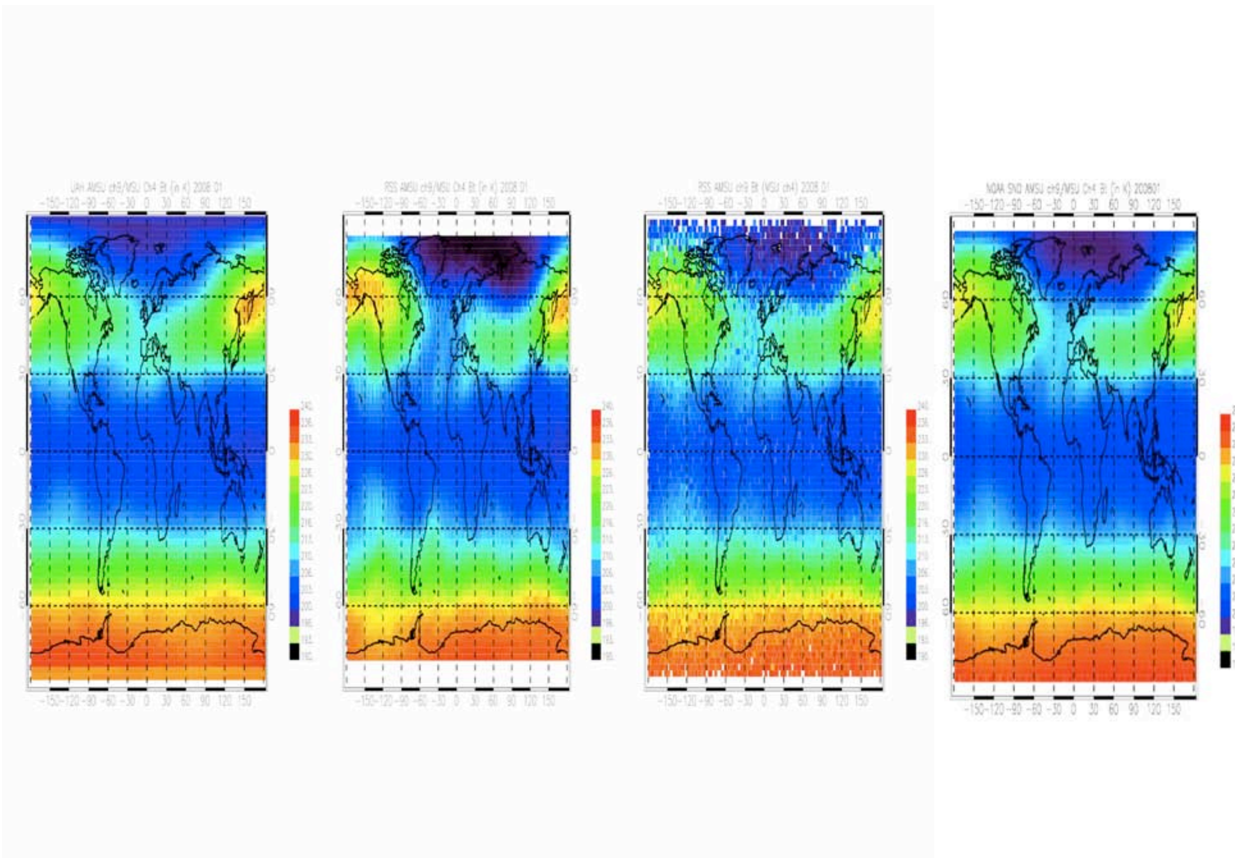

Figure 6. The monthly 2.5x2.5 gridded AMSU TLS for January, 2008 from UAH (the left panel), RSS (the second panel from the left), newly RO-calibrated TLS (the third panel from the left), and NOAA SNO TLS (the most right panel).

2.7 Comparisons of CHAMP/COSMIC, RSS, UAH, and SNO TLS Trends

Due to different adjustments and analysis procedures used to (a) correct satellite dependent bias, (b) correct geo-location dependent bias, (c) correct orbital drift dependent bias, and (d) merge data from different MSU/AMSU missions, significant differences were found among UAH, RSS, and SNO TLS tropospheric and stratospheric temperature trends. Since the adjustments are complicated and involve expert judgments that are hard to evaluate, the different temperature trends reported from different groups are still being debated. **In this study, we propose to use the RO-calibrated AMSU TLS to validate AMSU data processed by different groups and to understand exactly how and why there are differences in temperature trends reported by these analysis teams using the same observation systems but different analysis methods.**

a. *Comparisons over Lands and Oceans*

- **Quantify the mean biases among RSS, UAH, SNO, and RO calibrated AMSU monthly mean 2.5 degree $\times$2.5 degree TLS for one month:** here we compare AMSU TLS calibrated by high precision and geographically independent COSMIC TLS with those from RSS, UAH, and SNO over lands and oceans (**Figure 7**). This is to identify if the derived TLS from different centers are consistent over lands and oceans. **Figure 7** shows that SNO TLS is consistent with those of RO calibrated TLS over both lands and oceans with a mean bias of -0.56 K. Because UAH processes TLS (and other AMSU channels) over lands and oceans differently, UAH-RO TLS bias is very different for those over oceans (close to zero mean bias) from those over lands (about mean bias is equal to 0.6 K).

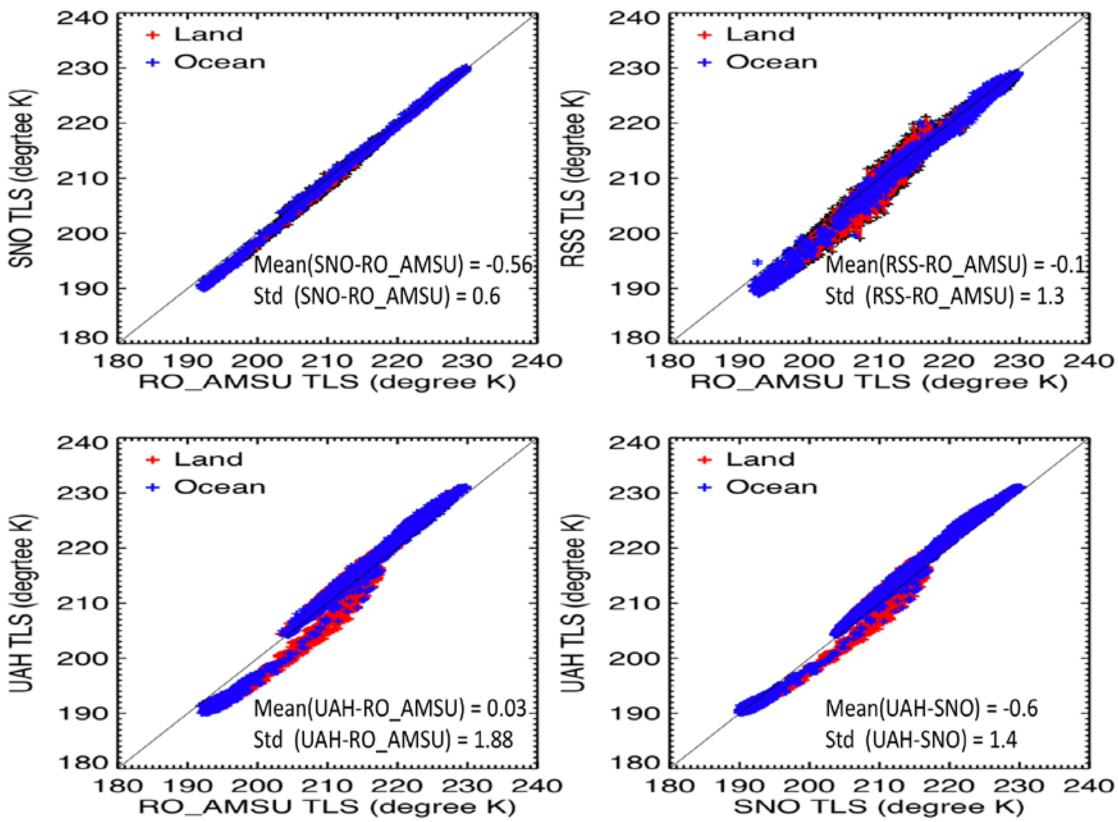

Figure 7. Comparisons of global monthly mean TLS in January, 2008 for each 2.5 degree×2.5 degree grid over lands (in red) and over oceans (in blue) between (a) SNO and RO calibrated AMSU (the upper left panel), (b) RSS and RO calibrated AMSU (the upper right panel), (c) UAH and RO calibrated AMSU (the bottom left panel), and (d) UAH and SNO (the bottom right panel).

b. Scattering plots of 10 x10 degree binned TLS from 200106 to 200812

- **Quantify the mean biases among RSS, UAH, SNO, and RO calibrated AMSU monthly mean TLS from 200106 to 200812:** to further compare all the RSS, UAH, SNO, and RO calibrated AMSU (RO_AMSU) TLS from 2001 06 to 2008 12, we first bin all the 2.5 degree x 2.5 degree TLS from the four groups into 10 degree x 10 degree TLS grids. Comparisons of monthly mean TLS in January, 2008 for each 10 degree×10 degree grid among RSS, UAH, and SNO and RO_AMSU is shown in **Figure 8**.
- **Figure 8** depicts the scattering diagrams of global monthly mean TLS for each 10 degree ×10 degree grid between RSS and RO_AMSU (the first panel), UAH and RO_AMSU (the second panel), SNO and RO_AMSU (the third panel), and RSS and UAH (the fourth panel).
- As shown in **Figure 8**, even though different calibration procedures were used, all RSS, UAH, and SNO TLS are highly correlated with RO_AMSU TLS (RO_AMSU_{TLS}). The correlation coefficients of RO_AMSU_{TLS}-RSS_{TLS} pairs, RO_AMSU_{TLS}-UAH_{TLS} pairs, and RO_AMSU_{TLS}-SNO_{TLS} pairs are all equal very close to 1.0. Consistent differences between RSS_{TLS} and RO_AMSU_{TLS} and between UAH_{TLS} and RO_AMSU_{TLS} are found. Although the difference between RO_AMSU_{TLS} and RSS_{TLS} is larger (RSS_{TLS} - RO_AMSU_{TLS} = -0.99K) than that between RO_AMSU_{TLS} and UAH_{TLS} (UAH_{TLS} - RO_AMSU_{TLS} = 0.02K), the standard deviation (Std) of RSS_{TLS}- RO_AMSU_{TLS} pairs (1.67 K) is smaller than that of UAH_{TLS}- RO_AMSU_{TLS} pairs (2.06 K). The mean bias of SNO_{TLS}-RO_AMSU_{TLS} pairs is equal to 0.5K where its standard deviation is as small as 0.5 K.

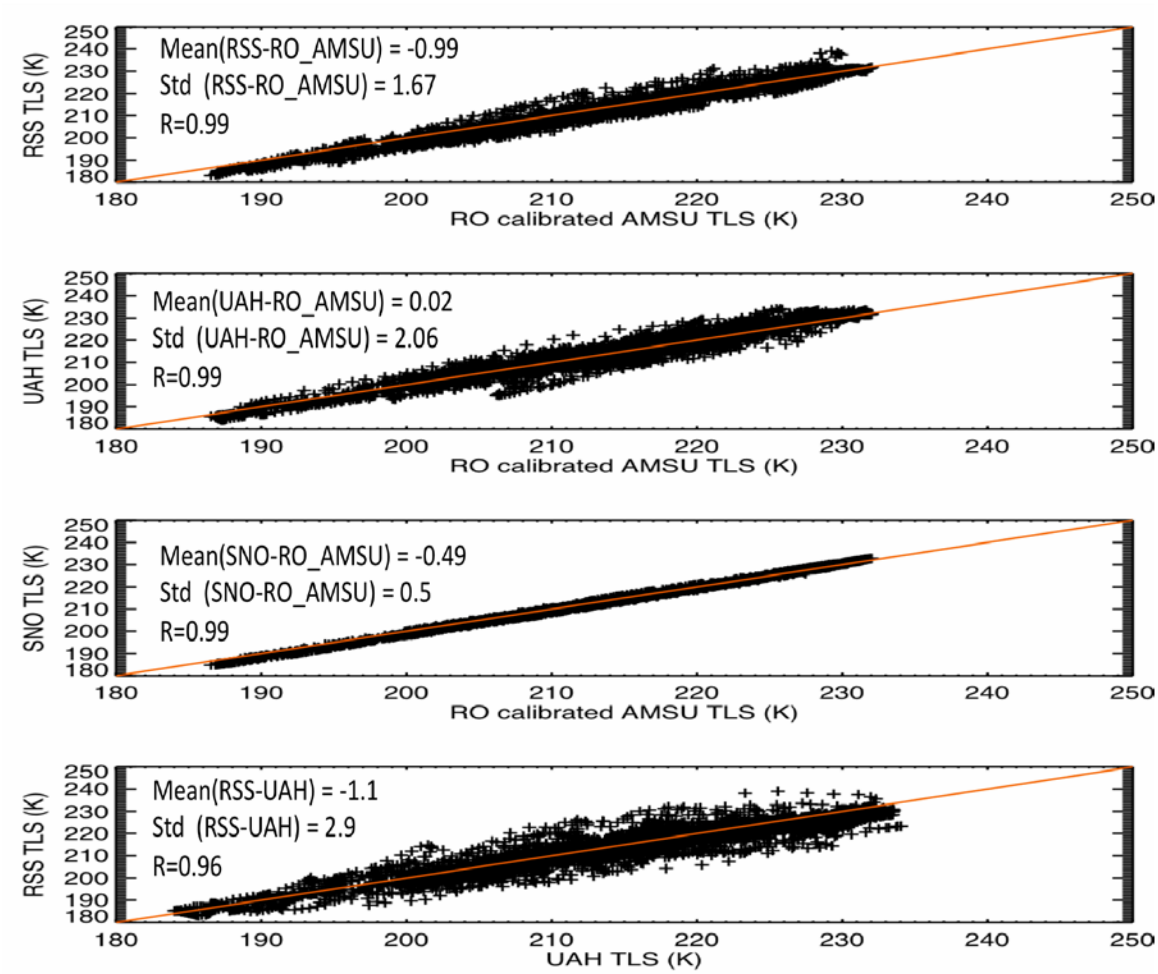

Figure 8. Scattering diagrams of global monthly mean TLS for each 10 degree $\times$10 degree grid between RSS and RO_AMSU (the first panel), UAH and RO_AMSU (the second panel), SNO and RO_AMSU (the third panel), and RSS and UAH (the fourth panel).

c. Time Series of TLS Difference

- **Quantify the time series of TLS difference:** To further quantify the time dependent anomalies among centers and understand the causes of the differences, we compute time series of TLS anomalies (in K) for RSS-RO_AMSU, UAH-RO_AMSU, and SNO-RO_AMSU pairs at six latitudinal zones (**Figure 9**) from 82.5º N to 82.5º S, 82.5º N to 60º N (northern high-latitudes), 60º N to 20º N (northern mid-latitudes and sub-tropics, further referred to as "mid-latitude" for brevity), 20º N to 20º S (Tropics), 20º S to 60º S (southern sub-tropics and mid-latitudes, further referred to as "mid-latitude" for brevity), and 60º S to 82.5º S (southern high-latitudes).
- The resulting curves are the centers' monthly retrieval differences from the monthly RO_AMSU TLS mean. Two qualitative features can be inferred from these figures: (1) individual centers' anomalies that are persistent in time, and (2) individual centers' anomalies that show large inter-monthly variance. For example, the global lower stratosphere (**Fig. 9a**) shows low inter-monthly variance of anomalies but a clear persistent anomaly for just one center. On the other hand, the northern high-latitude TLS (**Fig. 9b**) shows large inter-monthly variance in anomalies for UAH and RSS where SNO has a relative systematic anomaly.
- UAH shows a strong inter-monthly variance of anomalies over mid-latitudes and tropics.
- UAH, in particular, shows heightened anomaly variability (1 K) in mid-latitudes and tropics and northern and southern high latitudes, where the other SNO show less than 0.5 K.
- RSS shows large anomaly variability (-3 K) in the tropics and a 10 K anomaly in southern high-latitudes.

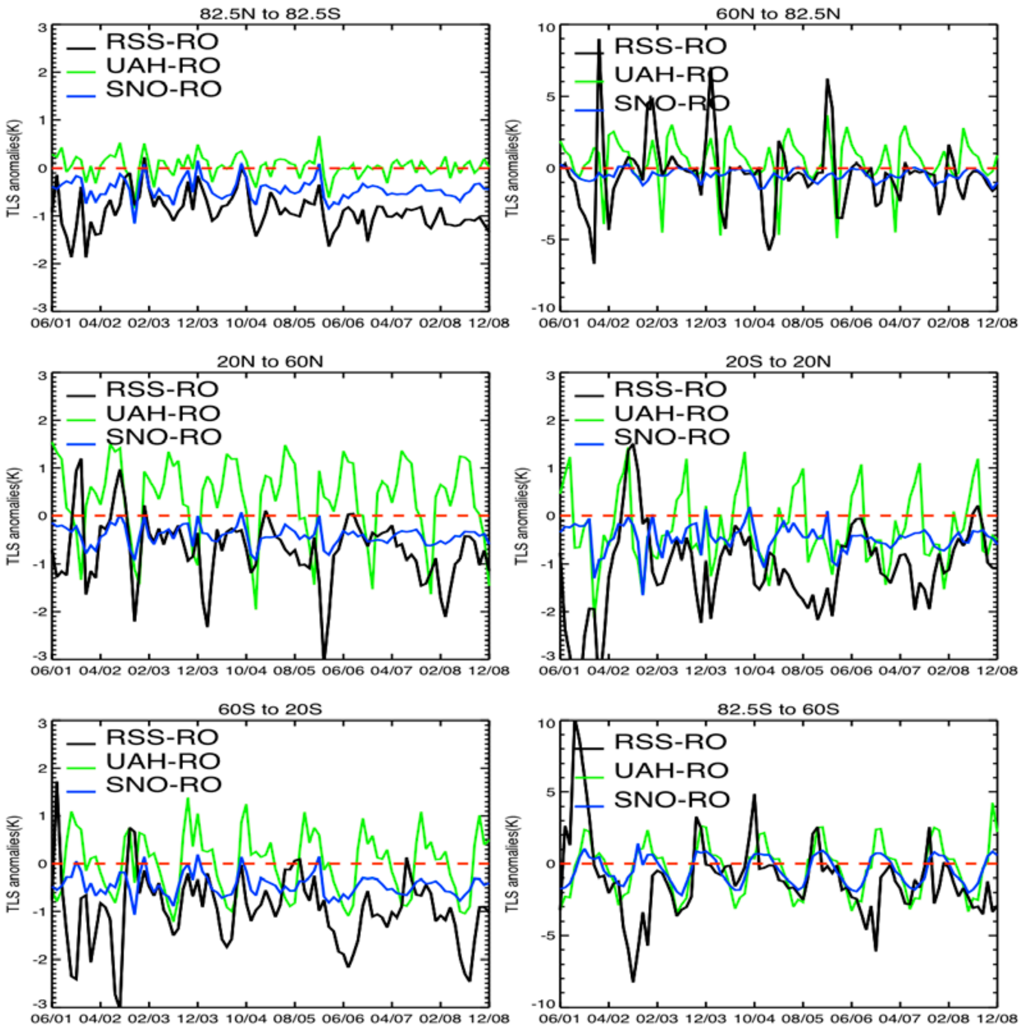

Figure. 9. The time series of TLS anomalies among four centers for the TLS for (a) the entire globe (82.5ºN-82.5ºS, the left upper panel), b) the 82.5ºN-60ºN zone (the upper right panel), (c) the 60ºN-20ºN zone (the middle left panel), (d) the 20ºN-20ºS zone (the middle right panel), (e) the 20ºS-60ºS zone (the bottom left panel), and (f) the 60ºS-82.5ºS zone (the bottom right panel). The RO_AMSU TLS mean was subtracted on a monthly basis.

d. Time Series of TLS Anomalies

To quantify the uncertainty of using MSU/AMSU data for climate monitoring, we examine the de-seasonalized TLS refractivity anomalies among four centers.

- **Trend analysis of time series of TLS anomalies:** The trend of TLS anomalies represents variation of atmospheric temperature in the lower stratosphere with time. **Figure 10** depicts RSS, UAH, SNO, and RO AMSU TLS time series anomalies for (a) the global (82.5˚ N to 82.5˚ S region), (b) 60˚ N to 82.5˚ N zone, (c) 20˚ N to 60˚ N zone, (d) 20˚ N to 20˚ S zone, (e) 20˚ S to 60˚ S zone, and (f) 60˚ S to 82.5˚ S zone. The best-fit linear trend (the slope of the linear fit) of each processing center is also generated.
- **Figure 10** shows that the time series of the TLS anomalies of the four centers vary with different latitudinal zones. Nevertheless, the trends in UAH, SNO and RO_AMSU agree within ±0.07 (K/5yrs) globally (see **Table 1**), because their differences are nearly constant in time. The trends for RSS are very different than others. More investigations will be followed in a near future.
- The regional trends estimates in the multi-center ensembles in the northern high-latitude, northern mid-latitude, Tropics, southern mid-latitude, and southern high-latitude upper troposphere are listed in **Table 1**.

From above analysis, we reach the following conclusions.

- The 0.02K-0.05 K precision of RO soundings are very useful to inter-calibrate AMSU/MSU data.
- The long-term stability of GPS RO data is very useful for climate monitoring.
- The RO calibrated AMSU TLS matches better with SNO and RSS in terms of variations (higher correlation coefficient) and matches better with UAH and SNO in terms of mean.
- The de-seasonalized TLS anomalies from UAH and SNO are, in general, agree well with that from RO calibrated AMSU Tb in all latitudinal zones. Small trend differences are found among SNO, UAH, and RO-calibrated AMSU.

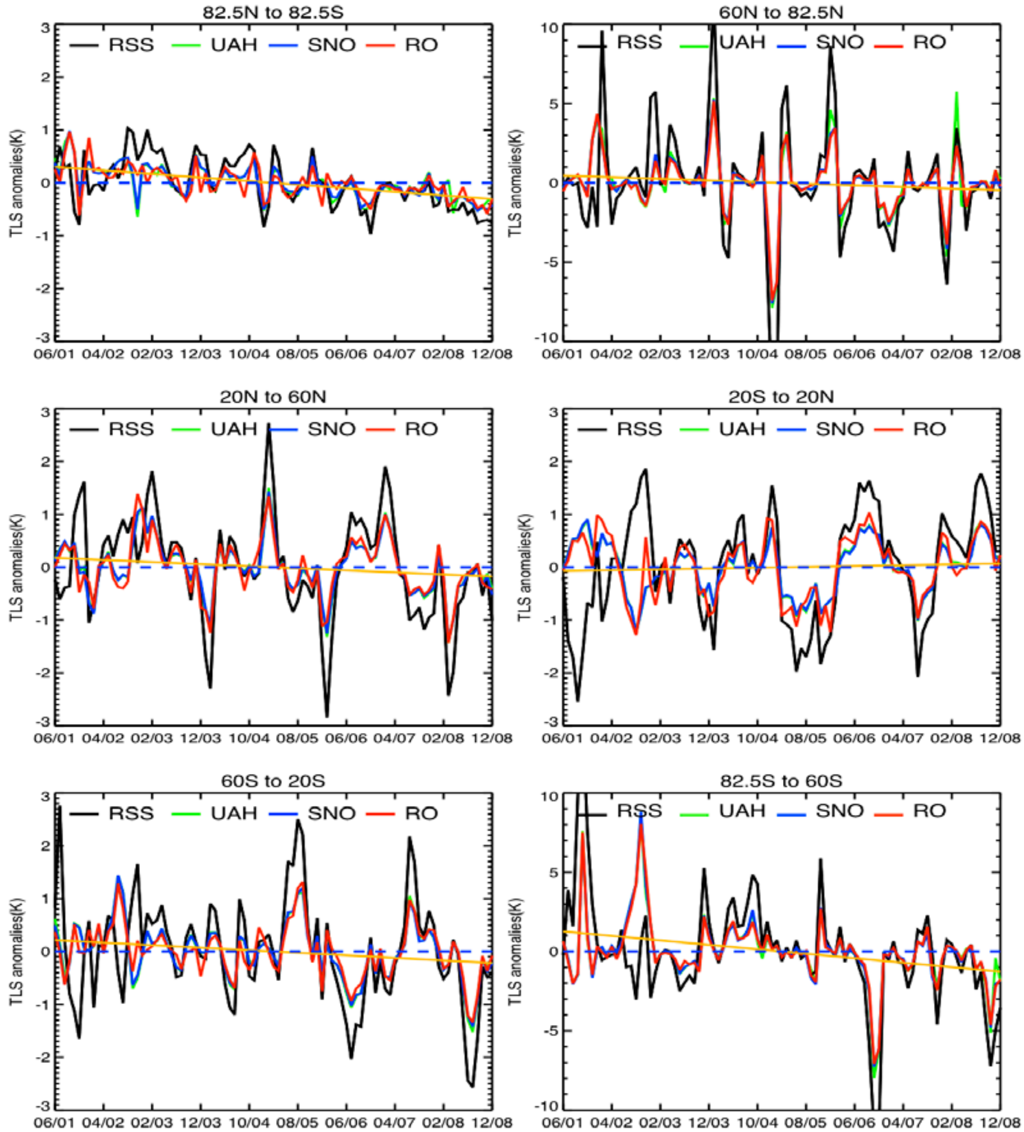

Figure 10. De-seasonalized lower stratospheric Tb anomalies of RSS, UAH. SNO, and RO_AMSU for (a) the entire globe (82.5ºN-82.5ºS, the left upper panel), b) the 82.5ºN-60ºN zone (the upper right panel), (c) the 60ºN-20ºN zone (the middle left panel), (d) the 20ºN-20ºS zone (the middle right panel), (e) the 20ºS-60ºS zone (the bottom left panel), and (f) the 60ºS-82.5ºS zone (the bottom right panel). The orange line indicates the mean trend for RO_AMSU.

	RSS	UAH	SNO	RO_AMSU	RSS-RO_AMSU	UAH-RO_AMSU	SNO-RO_AMSU
82.5°N-82.5° S	**-0.59**	**-0.46**	**-0.48**	**-0.41**	**-0.18**	**-0.05**	**-0.07**
60°N - 82.5° N	**-1.04**	**-0.67**	**-0.74**	**-0.62**	**-0.42**	**-0.05**	**-0.12**
20° N - 60° N	**-0.60**	**-0.30**	**-0.31**	**-0.24**	**-0.42**	**-0.06**	**-0.07**
20° N - 20° S	**0.55**	**0.07**	**0.05**	**0.1**	**0.45**	**-0.03**	**-0.05**
20° S - 60° S	**-0.52**	**-0.38**	**-0.37**	**-0.29**	**-0.23**	**-0.09**	**-0.08**
60°S - 82.5° S	**-3.22**	**-1.70**	**-1.80**	**-1.70**	**-1.52**	**0.0**	**-0.1**

Table 1 Trends for the period 200106-200812 of de-seasonalized lower stratospheric Tb anomalies (in K/5yrs) for RSS, UAH, SNO, RO_AMSU, RSS-RO_AMSU, UAH-RO_AMSU, and SNO-RO_AMSU for the global (82.5°N-82.5° S) and five latitudinal zones.

2.8 Publications and presentations

a. Refereed publications

(a) Papers published during this period

(1) **Ho, S.-P.**, M. Goldberg, Y.-H. Kuo, C.-Z Zou, W. Schreiner, 2009a: Calibration of Temperature in the Lower Stratosphere from Microwave Measurements using COSMIC Radio Occultation Data: Preliminary Results, Terr. Atmos. Oceanic Sci., Vol. 20, doi: 10.3319/TAO.2007.12.06.01(F3C).

(2) **Ho, S.-P.**, W. He, and Y.-H. Kuo, 2009b: Construction of consistent temperature records in the lower stratosphere using Global Positioning System radio occultation data and microwave sounding measurements, in New Horizons in Occultation Research, edited by A. K. Steiner et al., pp. 207–217, Springer, Berlin, doi:10.1007/978-3-642-00321-9_17.

(3) **Ho, S.-P.**, G. Kirchengast, S. Leroy, J. Wickert, A. J. Mannucci, A. K. Steiner, D. Hunt, W. Schreiner, S. Sokolovskiy, C. O. Ao, M. Borsche, A. von Engeln, U. Foelsche, S. Heise, B. Iijima, Y.-H. Kuo, R. Kursinski, B. Pirscher, M. Ringer, C. Rocken, and T. Schmidt, 2009c: Estimating the Uncertainty of using GPS Radio Occultation Data for Climate Monitoring: Inter-comparison of CHAMP Refractivity Climate Records 2002-2006 from Different Data Centers, J. Geophys. Res., doi:10.1029/2009JD011969.

(4) He, W., **S. Ho**, H. Chen, X. Zhou, D. Hunt, and Y. Kuo, 2009d: Assessment of radiosonde temperature measurements in the upper troposphere and lower stratosphere using COSMIC radio occultation data, *Geophys. Res. Lett.,* **36**, L17807, doi:10.1029/2009GL038712.

(b) Papers submitted during this period

(5) **Ho, S.-P.**, Ying-Hwa Kuo, Xinjia Zhou, and Doug Hunt, 2010a: Global Comparisons of the Radiosonde Water Vapor Measurements in the Troposphere using GPS Radio Occultation from COSMIC, *Remote Sensing* (accpeted).

(6) **Ho, S.-P.**, Ying-Hwa Kuo, 2010b: SI tracibility of RO data [In “States of the Climate in 2009]. *Bul. Amer. Meteor. Sci.*

(7) Mears C., Wang J., **Ho S.-P.,** Zhang L. and Zhou X., 2010c: Total Column Water Vapor, [In “States of the Climate in 2009]. *Bul. Amer. Meteor. Sci.*

(8) EOS, Peter Pilewskie, **S.-P. Ho**, etc 2009.

b. Scientific presentations

1) **Ho, S.-P.**, G. Kirchengast, S. Leroy, J. Wickert, A. J. Mannucci, A. Steiner, Y-H Kuo, C. Rocken, D. Hunt, W. Schreiner, S. Sokolovskiy, Quantitative Estimation of the Reproducibility of GPS RO Data for Climate monitoring: Inter-comparison of CHAMP Refractivity Climate Records 2002-2006 from Different Data Centers, European Geosciences Union annual meeting, Vienna, Austria, April 20-24, 2009.
2) **Ho, S.-P.**, Y-H Kuo, W He, D. Hunt, C. Rocken, W. Schreiner, and S. Sokolovskiy, Assessment of the Quality of Radiosonde Temperature and Water Vapor Measurements using GPS Radio Occultation from COSMIC, European Geosciences Union annual meeting, Vienna, Austria, April 20-24, 2009.
3) **Ho, S.-P.**, Y.-H. Kuo, D. Hunt, C. Rocken, W. Schreiner, S. Sokolovskiy, R. A. Anthes, and K. E. Trenberth, Applications of COSMIC Radio Occultation for Climate Monitoring, 2008 NOAA ESRL GLOBAL MONITORING ANNUAL CONFERENCE, May 14 and May 15, 2009, Boulder, CO.
4) **Ho, S.-P.**, et al., White paper for NCAR 5-year strategic plan: COSMIC – Providing GPS Atmospheric Remote Sensing Observations to Support NCAR's Missions in Weather, Climate and Ionosphere, Dec. 2008.
5) FORMAST-3 Evaluation Report and Follow-on Mission Plan, NSPO-PPT-004, 2009.
6) Ho et al., EGU.
7) **Ho, S.-P.**, Y.-H. Kuo, D. Hunt, C. Rocken, W. Schreiner, S. Sokolovskiy, R. A. Anthes, and K. E. Trenberth, Applications of COSMIC Radio Occultation for Climate Monitoring, 2008 NOAA ESRL Global Monitoring Annual Conference, May 14 and May 15, 2009, Boulder, CO.
8) **Shu-peng Ho,** Xinjia Zhou, Ying-Hwa Kuo, Doug Hunt, Chris Rocken, William Schreiner, and Sergey Sokolovskiy, Comparability of GPS Radio Occulation: inter-comparison of COSMIC, CHAMP, SAC-C, and GRACE-A Data, COSMIC Workshop, Boulder, CO., Oct. 27-29, 2009.
9) **Shu-peng Ho**, Xinjia Zhou, Ying-Hwa Kuo, Doug Hunt, Assessment of Systematic Biases of Radiosonde Temperature and Water Vapor Measurements using GPS Radio Occultation from COSMIC, COSMIC Workshop, Boulder, CO., Oct. 27-29, 2009.
10) Patrick Callagha, **Shu-peng Ho**, Thomas P. Yunck, Brian D. Wilson, Doug Hunt, Using COSMIC to Assess Accuracy of Temperature and Water Vapor Profiles from NCEP, ECMWF, AIRS under Cloudy Conditions, COSMIC Workshop, Boulder, CO., Oct. 27-29, 2009.
11) Wenying He, **Shu-peng Ho**, Hongbin Chen, Xinjia Zhou, Doug Hunt, Ying-Hwa Kuo, Assessment of Radiosonde Temperature Measurements in the Upper Troposphere and Lower Stratosphere using COSMIC Radio Occultation Data, COSMIC Workshop, Boulder, CO., Oct. 27-29, 2009.
12) **Shu-peng Ho**, Ying-Hwa Kuo, Chris Rocken, Xinjia Zhou, Doug Hunt, Construction of a Consistent Microwave Sensor Temperature Record in the Lower Stratosphere Using Global Positioning System Radio

Occultation Data and Microwave Sounding Measurements, AMS meeting, 2010.

13) Bill Schreiner, B. Kuo, C. Rocken, S. Sokolovskiy, D. Hunt, **S.-P. Ho**, X. Yue, T.-K. Wee, K. Hudnut, M. Sleziak-Sallee, T. VanHove. CDAAC Current Status and Future Plans. COSMIC workshop, Oct. 2009, Boulder, CO.
14) **Ho, S.-P.**, AMS meeting 2010: Global Comparisons of Atmospheric Soundings in the Lower Troposphere from COSMIC Radio Occultation, Radiosonde, and ECMWF Analysis
15) **Ho, S.-P.**, Applications of COSMIC RO to Climate Studies, the third CMOS/CGU meeting, May 31 – June 4, Ottawa 2010 (invited talk).
16) **Ho, S.-P.,** NASA-CVO project review, Washington D.C., 2009/12/03
17) **Ho, S.-P.,** Presentation in COSMIC retreat: COSMIC scientific applications
18) **Ho, S.-P.**, NOAA SDS PI report, NCDC, Sept. 2009.
19) **Ho, S.-P.,** NOAA MSU/AMSU/SSI workshop, April 2010
20) **Ho, S.-P.,** Tele-conference presentation: JPL talk about the "Enhancement of the AIRS Troposphere and Stratosphere Temperature Climate Data Records using Global Positioning System Radio Occultation Data"

3. Immediate Plans for the Remainder of Calendar Year 2009

Since we have completed the

1) Preparation of GPS RO, Radiosonde data,
2) MSU/AMSUMOPITT data for Geo-location Comparisons"
3) Testing and refining the methods to use GPS RO data to inter-compare and inter-calibrate MSU/AMSU data",
4) Construction of a consistent microwave sensor temperature record in the lower stratosphere using GPS RO data and microwave sounding measurements",
5) Comparisons of CHAMP/COSMIC, RSS, UAH, and SNO TLS Trends",

immediate plans for the remainder of this calendar year (from May to July 2010) will include

1) Preparation of manuscripts to summarizing results described above,
2) Using temperature profiles from RO-identified radiosondes to calibrate MSU/AMSU brightness temperatures in the troposphere,
3) Generating long-term stratospheric and tropospheric climate quality temperature datasets by reprocessing nine years of AMSU/MSU data from 2001 to 2009.
4) Documenting details of analysis codes and data used to generate the consistent microwave sensor temperature record in the lower stratosphere and troposphere using GPS RO data and microwave sounding measurements.

4. Plans after July 2010 (year 4 of this study)

After July 2010, we plan to work with identified NCDC personnel who is an assumed export in GPS RO and MSU/AMSU data to transfer the UCAR data and computer codes for generating the consistent microwave sensor temperature record in the lower stratosphere and troposphere to NCDC. Again, due to the evolving nature of this study and practical difficulties to transfer the analysis codes from UCAR to NCDC, we propose to extend these processes into year 4 of the project. This is to ensure RO/MSU/AMSU/radiosnde data and the analysis and processing computer codes can be completely transferred so that these codes can re-produce the microwave temperature data records over NCDC just as over UCAR. We plan to start to work with NCDC experts as soon as they are identified.